Methods of Calculating Moisture Discharge Characteristics of Insulators

Shevchenko S., Danylchenko D., Hanus R., Radohuz S., Tomashevskiy R., Makhonin M., Potryvai A.
National Technical University «Kharkiv Polytechnic Institute»
Kharkiv, Ukraine

Abstract. The article discusses methods for calculating the moisture discharge voltage of insulators under various operating conditions (pollution, humidity, etc.) to identify patterns of environmental influence on operational characteristics, as well as to improve the reliability and safety of power grids. The main aim of the study is to compare two approaches to calculating the moisture discharge characteristics of insulators: the classical method based on the Tepler formula and an alternative approach that utilizes generalized parameters. These parameters can be easily obtained from the technical characteristics of insulators or design standards for automated calculations. To achieve this goal, the authors addressed several important tasks. First, a comprehensive analysis of the behavior of electrical discharges on the surface of insulators under various operating conditions, including standard and adverse environments, was conducted. Second, an automated tool was developed to quickly and accurately determine the values of moisture discharge voltage. Third, the proposed method was experimentally validated using the LK 70-110 insulator. The tests revealed a discharge voltage of 549 kV and an electric field intensity of 2.1 kV/cm, confirming the accuracy of the calculation method. The key findings of the study highlight the importance of considering factors such as the properties of insulator surfaces and the degree of contamination, especially in underground substations where humidity and pollution exhibit specific characteristics. The proposed approach proved effective both in standard and challenging operating conditions. The significance of the results lies in the creation of a tool that simplifies the calculation of moisture discharge characteristics of insulators.
Keywords**:** moisture discharge voltage, insulators, calculating method, Tepler's formula, electrical discharges, automated calculator.

DOI: https://doi.org/10.52254/1857-0070.2025.1-65.11
UDC: 621.315.623

Metode de calcul a tensiunii de descărcare la umiditate a izolatoarelor

Șevcenco S., Danilicenco D., Ganus R., Radoguz S., Tomașevsky R., Mahonin N., Potrâvai A.Ă.
Universitatea Națională Tehnică „Institutul Politehnic din Kharkiv” Harkov, Ucraina

Rezumat. Acest studiu investighează metode de determinare a tensiunii de descărcare a umidității izolatoarelor, subliniind aplicarea acestora în îmbunătățirea fiabilității și siguranței rețelei electrice. Cercetarea se concentrează pe analiza comportamentului de descărcare de-a lungul suprafețelor izolatoare în diferite condiții, cu o atenție deosebită la două abordări de calcul. Prima metodă utilizează formula clasică Teppler, care necesită date experimentale. A doua, o alternativă nouă, se bazează pe parametri generalizați, permițând calculul automat. Constatările cheie includ validarea cu succes a metodei alternative împotriva formulei Teppler prin testarea pe izolatorul LK 70-110, care a demonstrat tensiuni de descărcare de 549 kV și niveluri de stres de 2,1 kV/cm. Această metodă s-a dovedit eficientă atât în scenarii de mediu standard, cât și nefavorabile. Mai mult, dezvoltarea unui instrument automat de calcul facilitează determinarea rapidă și precisă a caracteristicilor de descărcare umedă, oferind avantaje practice pentru proiectarea și întreținerea izolației. Cercetarea evidențiază rolul critic al proprietăților suprafeței izolatorului și al contaminării în influențarea comportamentului de descărcare. Subliniază necesitatea unor soluții de izolare adaptate pentru diferite medii operaționale, inclusiv substații subterane, unde condiții precum umiditatea și tipul de contaminant diferă semnificativ. Abordarea propusă oferă un cadru inovator pentru îmbunătățirea performanței izolației, contribuind la dezvoltarea rețelelor electrice mai sigure și mai eficiente.
Cuvinte-cheie**:** tensiune de descărcare la umiditate, izolatori, metode de calcul, formula lui Toepler, descărcări electrice, calculator automat.

Методики расчета влагоразрядного напряжения изоляторов

Шевченко С.Ю., Данильченко Д.О., Ганус Р.О., Радогуз С.А., Томашевский Р.С., Махонин Н.В., Потрывай А. Э.

Национальный технический университет «Харьковский политехнический институт»

Харьков, Украина

Аннотация. В статье рассматриваются методы расчета влагоразрядного напряжения изоляторов в различных эксплуатационных условиях (загрязненность, влажность и т.п.) с целью выявления закономерностей влияния окружающей среды на эксплуатационные характеристики, а также повышения надежности и безопасности электрических сетей. Основная цель исследования заключается в сравнении двух подходов к расчету влагоразрядных характеристик изоляторов: классического метода, основанного на формуле Теплера, и альтернативного способа, использующего обобщенные параметры, которые довольно просто получить из технических характеристик изоляторов или норм по проектированию, для автоматизированных расчетов. Для достижения этой цели авторы решили ряд задач. Во-первых, был проведен всесторонний анализ поведения электрических разрядов на поверхности изоляторов при различных условиях эксплуатации, включая стандартные и неблагоприятные среды. Во-вторых, разработан автоматизированный инструмент, способный быстро и точно определять значения влагоразрядного напряжения. В-третьих, проведена экспериментальная проверка предложенного метода с использованием изолятора ЛК 70-110. Испытания показали разрядное напряжение 549 кВ и напряженность 2,1 кВ/см, что подтверждает точность расчетного метода. Основные результаты исследования подчеркивают значимость учета таких факторов, как свойства поверхностей изоляторов и степень их загрязнения, особенно в условиях подземных подстанций, где влажность и загрязнения имеют специфические особенности. Предложенный подход оказался эффективным как в стандартных, так и в сложных эксплуатационных условиях. Значимость результатов заключается в создании инструмента, который упрощает расчет влагоразрядных характеристик изоляторов, что позволяет быстро смоделировать ряд различных эксплуатационных условий и выбрать оптимальные характеристики для изоляторов. Этот метод может быть использован для разработки индивидуальных решений, адаптированных к различным условиям эксплуатации, что способствует быстрому моделированию и, соответственно, более точному определению безопасных и эффективных решений. Работа делает вклад в улучшение характеристик изоляции и открывает новые возможности для исследований и практического применения в энергетике, в частности в подземных подстанциях.

Ключевые слова: влагоразрядное напряжение, изоляторы, методики расчета, формула Теплера, электрические разряды, автоматизированный калькулятор.

INTRODUCTION

Insulators play a crucial role in electrical networks, ensuring the separation of conductive parts and maintaining their functionality even under difficult operating conditions.

One of the most common problems encountered in their application is the so-called "moisture discharge" phenomenon [1-4].

Moisture discharge voltages can significantly reduce the efficiency of insulation, leading to malfunctions in electrical systems.

A key aspect in the design of reliable insulation systems is therefore the correct calculation of these voltages [4-7]. This articles analyses and compares two different methods for calculating the wet discharge voltage. In particular, it assesses their practical applicability and accuracy for use in underground substations.

DISCHARGE IN THE AIR ALONG THE SURFACE OF THE INSULATORS

Let's examine how a solid dielectric influences the initiation and progression of an electrical discharge across the surface of an insulator in air. In the case of the structure shown in Figure 1a, the electric field lines are parallel to the dielectric surface and the field is homogeneous. In the structure (Figure 1b), the field is inhomogeneous and the tangential component of the field strength on the dielectric surface $E\tau$ prevails over the normal component En. In the structure (Figure 1c), the field is also inhomogeneous, but the normal component prevails. The first design is comparatively rare in real life, but it is convenient for detecting the influence of dielectric characteristics on the occurrence of discharge, while the second and third designs are quite common (reference and pass-through insulators). [8-13]

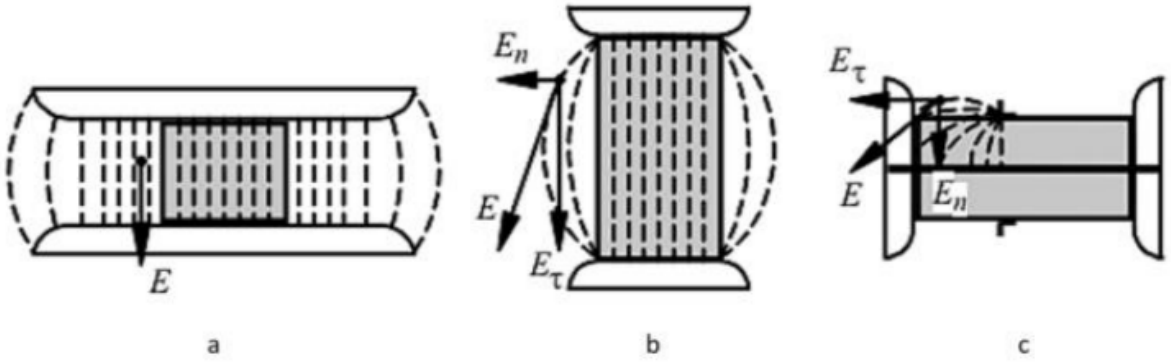

Fig. 1. Typical designs of solid dielectric air gaps. [1]

In an insulating construction, the electrical strength of the dielectric gap is lower than that of the purely air gap. This is due to the adsorption of moisture from the ambient air on the surface of the dielectric as well as to the micro-gaps between the solid dielectric and the electrode. The surface of all bodies in humid air is covered with a thin film of water. Ions formed in this film under the influence of an electric field move towards the electrodes. As a result, the field near the electrodes is strengthened, and in the middle of the gap it is weakened. The strengthening of the field near the electrodes leads to a decrease in the electrical strength of the gap. This decrease is greater the more hydrophobic the dielectric is. For example, glass is a more hygroscopic material than glazed porcelain, so the flashover stress along the glass surface will be less than along the porcelain. A decrease in the insulator flashover voltage in the presence of a microgap between the dielectric and the electrode or a microcrack on the surface of the dielectric is associated with an increase in field strength due to the difference in dielectric constant between air and a solid dielectric (the dielectric constant of a solid dielectric is 3-4 times higher than that of air). Increasing the field strength to the microgaps leads to ionization processes. The products of these ionization processes (ions and electrons), which fall into the main gap, create a local field enhancement, which leads to a decrease in the flashover voltage. To increase the discharge voltage of the gap with a solid dielectric, it is necessary to use low-humidity dielectrics or to create a coating of low-humidity materials that protect the dielectric from contact with water vapor (for example, glazing the surface of porcelain), as well as to ensure a reliable, micro-gap-free connection of the insulator body to the metal reinforcement using cement embedded and elastic conductive gaskets. In the insulating structure (Figure 1b), the field is not homogeneous, so, as in the case of a purely air gap, the discharge voltage is lower than in a homogeneous field. The influence of the hygroscopically of the dielectric and the microgaps is qualitatively the same as in the design in Figure 1a, but it is less pronounced because the electric field is already significantly inhomogeneous. If the field is sufficiently inhomogeneous, a corona discharge will occur in this insulating structure, just as in a pure air gap. The resulting ozone and nitrogen oxides attack the solid dielectric [14-18]. The corona discharge is most dangerous for polymeric insulation, especially if it is in the form of a streamer. The temperature in the streamer channel is quite high, and its contact with the surface of the dielectric can lead to thermal decomposition of the dielectric and the formation of a charred track of increased conductivity. The length of this track increases over time, leading to the flashover of the insulator with an irreversible loss of electrical strength. All of the above also applies to the structure in Figure 1c. The large normal component of the electric field brings the streamer channel closer to the dielectric surface, increasing the likelihood of dielectric damage. The electrical strength of this structure is even lower than that in Figure 1b. The streamer channels developing along the dielectric surface have a much higher capacitance relative to the internal (opposite) electrode than in the design with a predominant tangential field component. Therefore, a relatively large current flows through the streamer channels. At a certain voltage, the current increases to the point where the temperature of the streamer channels becomes sufficient for thermal ionization. A thermally ionized discharge channel that develops along a dielectric at the surface of which the normal component of the field strength exceeds the tangential component is called a sliding discharge channel. The conductivity of the sliding discharge channel is much higher than the conductivity of the streamer channel, therefore the voltage drop in the sliding discharge channel is less, and on the unobstructed part of the gap - more than in the streamer channels. An increase in the voltage on the nonflashovered part of the gap leads to a lengthening of the sliding discharge channel and complete flashover of the gap at a lower value of the voltage between the electrodes. The length of the sliding discharge channel depends on its conductivity and therefore on the value of the current in it. In turn, the current depends on the voltage between the

electrodes, the change in voltage, and the capacity of the streamer channel relative to the opposite electrode. The influence of these parameters is reflected in Teppler's empirical formula for the length of the sliding discharge channel [4, 19-20]:

$$l_{slide} = \chi_1 \cdot C^2 \cdot U^5 \sqrt[4]{\frac{dU}{dt}} \qquad (1)$$

where χ_1 is the experimentally determined coefficient; C – is the specific surface capacitance (capacitance of the dielectric surface at which the discharge develops relative to the opposite electrode); U – is the applied voltage. From formula (1), if the distance between the electrodes on the surface of the dielectric is replaced by l_{slide}, it is possible to determine the value of the voltage UP required to flashover the insulator. If we take $C = \frac{\varepsilon \cdot \varepsilon_0 \cdot S}{d}$, where d – is the thickness of the dielectric and the area S is taken to be equal to 1 cm^2, and if we consider the value dU/dt to be constant, which in a first approximation corresponds to the constant frequency of the applied voltage, we obtain from formula (1) the equation for finding the discharge voltage, which is called the Teppler formula:

$$U_p = \chi \cdot L^{0,2} \left(\frac{d}{\varepsilon \cdot \varepsilon_0}\right)^{0,4} \qquad (2)$$

It follows from Teppler's formula that increasing the length of the insulator gives a relatively small increase in the discharge voltage. Therefore, to increase the discharge voltages of pass-through insulators, the specific surface area is reduced by increasing the diameter of the insulator near the flange from which the discharge can be expected. They also employ a semiconductor coating near the flange, which aids in equalizing the voltage distribution across the insulator's surface, thereby raising the discharge voltage levels. At a constant voltage, the specific surface capacitance has practically no effect on the development of the discharge. The value of the discharge voltage is found to be close to the discharge voltage of a pure air gap.

DISCHARGE ALONG CONDUCTIVE AND CONTAMINATED INSULATOR SURFACE

In typical operating environments, insulator surfaces are continually subjected to contamination. Dry contaminants, which have high resistance, typically have little impact on the voltage distribution across the insulator's surface and thus do not substantially lower the discharge voltage. However, when these contaminants are wetted by light rain or dew, their resistance drops, causing a redistribution of voltage across the insulator, which in turn significantly reduces the discharge voltage.

The mechanisms at work when an insulator is exposed to rain and when its surface is both dirty and wet share similarities. Let's analyze how a discharge develops when the insulator's surface is both dirty and wet.

Intensive drying of the insulator surface near arc ends causes them to extend. When the entire surface dries, the leakage current decreases, and the partial arcs grow as they lengthen. If drying results in a reduced leakage current, the arcs will extinguish. Conversely, if the leakage current rises, the partial arcs will continue to extend and eventually span the entire insulator. Because the characteristics of partial arcs and the number of arcs on the insulator surface are unpredictable, complete arc coverage is a random event with a certain probability. This probability increases with higher operating voltage, as it boosts the leakage current, encouraging the extension of partial arcs until the insulator is fully covered. The depicted discharge behavior suggests that insulators will have higher discharge voltages when the leakage current is minimized [21-23].

$$I_l = \frac{U}{R_l} \qquad (3)$$

where I_l is the insulator leakage current.

R_l – is the leakage resistance on the surface of the insulator.

For a cylindrical smooth insulator with a diameter D, if the contamination layer has a thickness Δ and a specific volume resistance ρ, then.

$$R_l = \frac{\rho \cdot L_l}{\pi \cdot \Delta \cdot D} \qquad (4)$$

where L_l – the path length of the leakage current. From formulas (3) and (4) it follows that

$$I_l = \frac{U \cdot \pi \cdot \Delta \cdot D}{\rho \cdot L_l} \qquad (5)$$

Therefore, as the leakage path length increases and the insulator diameter decreases, the insulator discharge voltage increases:

$$U_{MD} = \frac{I_l \cdot \rho \cdot L_l}{\pi \cdot \Delta \cdot D} \qquad (6)$$

Since the drying of the insulator surface is relatively slow, it does not significantly impact short-term overvoltages, resulting in a higher flashover voltage compared to longer-term voltage exposure. The wet discharge voltage of an insulator is contingent upon various factors, including the characteristics of the contaminant layer—such as its

amount, composition, and the extent of wetting. Due to the wide range of contamination types encountered in practical scenarios, defining a single "standard" contamination for wet discharge voltage assessment is difficult. Therefore, precise measurements of discharge voltages under real-world dirt and moisture conditions are best derived from operational experience.

For theoretical design optimization, the wet discharge voltage can be analyzed by considering factors such as the length of the leakage current path along the insulator surface between electrodes (L_{fl}), the insulator's design, rain characteristics, and the voltage type. Testing should be conducted with the insulator in its normal operational position, rain applied at a 45° angle to the horizontal at a rate of 3 mm/min, and the water's conductivity set to 10-4 S/cm. Voltage should be applied 5 minutes after the wetting begins (Figure 2).

In cases where the rib protrusion is minimal (a/1 < 0.5), the wet discharge voltage tends to increase due to the extended dry regions beneath the ribs. Consequently, the discharge primarily traverses along the rib surfaces.

An increase in l (with a remaining constant) will lead to a decrease in U_{MD} because the dry zones beneath the ribs become smaller. Therefore, l should be minimized. Practical experience indicates that under typical conditions, the ratio *a/l* should not exceed 0.5.

It is recommended to increase the a/l ratio to 0.8-1.0 when operating the insulator in polluted conditions.

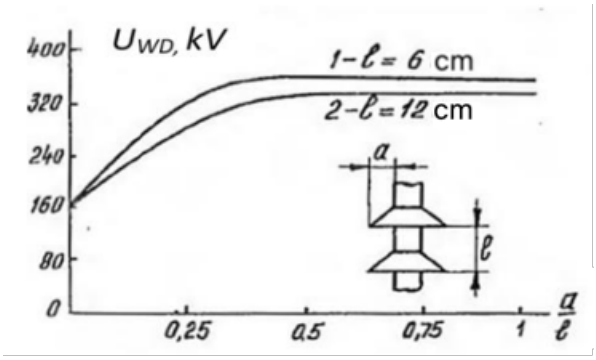

Fig. 2. Dependence of U_{MD} on *a/l* of insulator.

The ribs are typically inclined at an angle of approximately 15-25° [24-26]. When a > 30 mm, the effect of the rib angle on U_{MD} is minimal. To avoid water from wetting the underside of the rib and diminishing the dry areas on the insulator surface, a drip feature must be incorporated into the rib design (see Figure 3). For an industrial frequency voltage and a rain rate of 5 mm/min, the minimum wet discharge voltage can be calculated using the formula $U_{MD}=2.15l_{DD}$ kV, where l_{DD} is measured in centimeters.

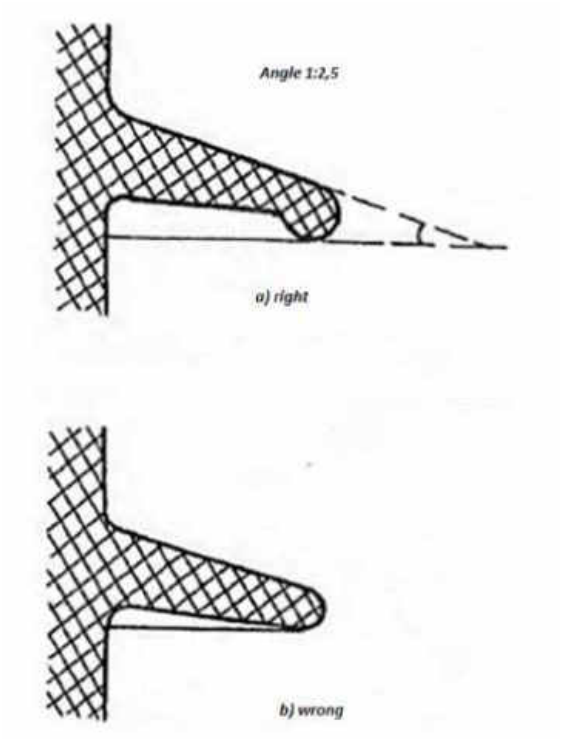

Fig. 3. Rib profile.

Moisture discharge voltages for both constant and alternating currents are essentially equivalent. Atmospheric conditions, such as pressure and temperature, have minimal impact on U_{MD}. Although rain does not directly affect underground power lines, general humidity and condensation still play a role. Typically, higher water conductivity in the form of aerosols, whether in the air or on surfaces, leads to a lower U_{MD}. Impulse discharge voltages along the surface of a dielectric are largely unaffected by rain and moisture. For a frequency of 50 Hz, the average moisture discharge voltage ranges from 2.1 to 2.4 kV/cm. When selecting insulation for areas prone to contamination, the key parameter is the specific length of the leakage path (l_{sl}), defined as the ratio of the total leakage path length (L_{fl}) to the maximum operating linear voltage (U_{wl}).

ALTERNATIVE CALCULATION METHOD

Despite the validity of the above method, the described formulas have parameters that are difficult to set or impossible without an experiment, so the above method can be used as a means of checking the results of the experiment. [27-31]

However, before the experiment, we need to establish the calculation data.

Let's recall that the flashover of the insulation usually occurs when it is wetted by drizzle, mist or dew, when the contaminated layer is saturated with moisture and an electrolyte appears on the surface of the insulators. A current begins to flow along the surface of the insulator, known as the leakage current [32, 33]. The electrolyte heats up and the moisture

evaporates. Dry zones appear in certain areas of the surface where the current density is greatest, or the thickness of the wetted layer is smallest. These zones expand rapidly in the direction perpendicular to the current lines until, due to the increase in voltage drop, the dried zones flashover to a width of only a few millimetres in the air. An electric arc is formed, the reference points of which are located at the edges of the dried zone. The volt-ampere characteristic of the arc corresponds to the function of the species

$$E_a = al^{-n} \tag{7}$$

where a and n are constants that depend on the current and air density.

The current flowing through the arc channel is limited by the surface resistance of the insulator. The surface resistance of a smooth rod insulator with a diameter d with a leakage current path length L and a contamination layer thickness Δ is equal to [34,35].

$$R_S = \rho_v \frac{L}{\pi \Delta D} = \frac{\rho_S L}{\pi D} = \frac{L}{\pi \gamma_S d} = \frac{L}{\gamma_S B} \tag{8}$$

where πΔD is the cross-sectional area of the pollution layer;

ρ_v – its specific volume resistance;

ρ_s – specific surface resistance;

γ_s – specific surface conductivity;

B – the width of the flow path of the leak.

The determination of Rs by surface resistivity or conductivity is more convenient as it does not require knowledge of values that are difficult to determine - the thickness of the contamination layer. [36-39]

The resistance of the contamination layer partially shunted by the arc:

$$R_\Sigma = R_S - (r_S - r_a) l_a \tag{9}$$

where r_s and r_a – resistance per unit length of insulator surface and arc; l_a – the length of the arc.

According to formulas (5) and (6)

$$r_S = \frac{1}{\pi \gamma_S d} = \frac{1}{\gamma_S B} \tag{10}$$

$$r_a = \frac{E_a}{l} = al^{-(n+1)} \tag{11}$$

If at the point of origin of the dried annular zone $r_s > r_a$, where r_s is the resistance of the section under consideration in the wetted state, then after the arc $R_\Sigma < Rs$ and the surface current of the insulator when the arc occurs decreases compared to the current on the wetted surface.

$$I = \frac{U}{R_\Sigma} = \frac{U}{R_s - (r_s - r_a) l_a}. \tag{12}$$

The wet surface, heated by the support points of the arc, dries quickly. The arc therefore moves continuously. As a result, the dried annular zone expands, causing the arc to elongate. Consequently, the current decreases according to equation (9), which increases the resistance r_a, further reducing the current. This process reduces the heat dissipation at the insulator surface, causing it to become wet again. As a result, the current returns, and the arc is extinguished. This cycling of drying and wetting is a normal operational behavior for insulation in electrical networks [40]. Also, if $r_s < r_a$, then $R_\Sigma < R_s$ and the current increases after the arc. As the arc spreads, the resistance r_a decreases further and the current increases. This in turn leads to a further decrease in resistance r_a and a further increase in current. As a result, the support points of the arc slide across the wetted surface at a speed of 50 m/s or more until the insulator is completely covered. Based on the above, the flashover condition of the insulator is completely covered.

Based on the above, the flashover condition of the insulator is

$$r_a \le r_s \tag{12}$$

Which when substituting the values of rs and ra will be rewritten in the form

$$al^{-(n+1)} \le \frac{1}{\pi \gamma_s d} = \frac{1}{\gamma_s B} \tag{13}$$

When $r_s = r_a$ we get the limiting current on the surface of the insulator

$$I_{ls} = (\alpha \gamma_S \pi d)^{1/(1+n)} = (\alpha \gamma_S B)^{1/(1+n)} \tag{14}$$

At this and higher currents the insulator flashovers. Using this current limit, we obtain the moisture discharge voltage

$$U_{MD} = I_{ls} R_s = \frac{La^{1/(1+n)}}{(\gamma_S \pi d)^{n/(1+n)}} = \frac{La^{1/(1+n)}}{(\gamma_S B)^{n/(1+n)}} \tag{15}$$

As can be seen, UMD is proportional to the length of the leakage path, which allows us to determine the average moisture discharge stress along the length of the leakage path which decreases with increasing insulator diameter and surface conductivity (Fig. 4). [33].

$$E_{MDL} = \frac{U_{MD}}{L} = \frac{a^{1/(1+n)}}{(\pi \gamma_S d)^{n/(1+n)'}} \tag{16}$$

At the same time, the leakage current limit increases as the diameter of the insulator increases. Calculations were made using formulas (14) and (15) with a = 1.4 · 104 V·An /m, n = 0,56. Based on this, for small γs, the discharge voltages at d < 4 cm are sufficiently high.

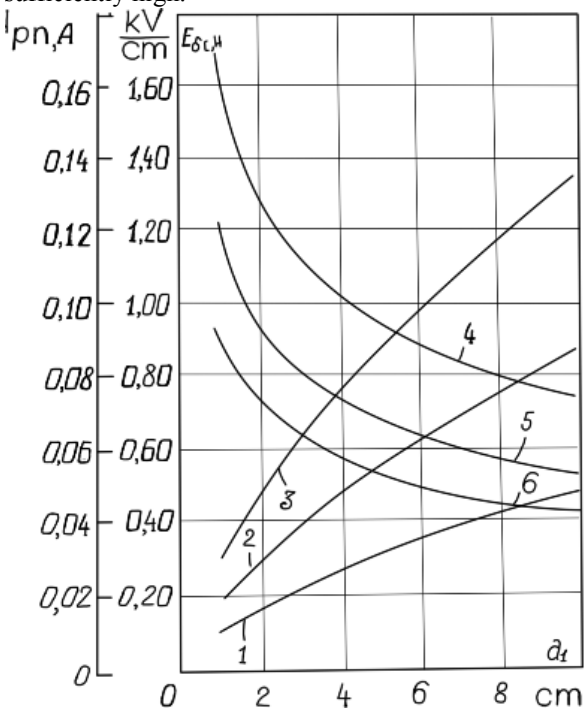

Fig. 4. Dependencies of the limiting leakage currents (curves 1, 2 and 3) and minimum discharge field strengths along the path of the leakage stroma (curves 4, 5 and 6) of cylindrical insulators on the diameter of the insulator at different conductivities, the limits and values of which were determined in laboratories empiricallyand mapped in standards such as the RDE (ПУЭ): γs = 2 μSm (curves 1, 4); 5 μS (curves 2, 5); 10 μS (curves 3 and 6) [36].

However, as the diameter of the insulator and the degree of its contamination increase, EMD L decreases to such an extent that it is impossible to create an acceptable insulating structure for outdoor equipment [41]. To increase the discharge voltages, ribs are used (Fig. 5), whose role is reduced to increasing the resistance per unit of insulator height. With the same γs for the bar and the rib, the resistance of the wetted surface of a rib (its two sides and its outer edge) is

$$R_s = \frac{2}{\pi\gamma_s}\int_0^{0,5(d_2-d_1)}\frac{dl}{d(l)} + \frac{c}{\pi\gamma_s d_2'} \quad (17)$$

where l – is the current coordinate along the leakage path, counted from the place where the rib meets the rod. Since d(l) = d1 + 2l cosα, dd(l) = 2 cosα dl (Figurte 5), then, moving to the variable d and changing the limits of integration accordingly, we obtain d(l) = d1 at l = 0, d(l) = d2 at l = 0,5 (d2 – d1)

$$R_s = \frac{1}{\pi\gamma_s \cos\alpha}\ln\frac{d_2}{d_1} + \frac{c}{\pi\gamma_s d_2} \quad (18)$$

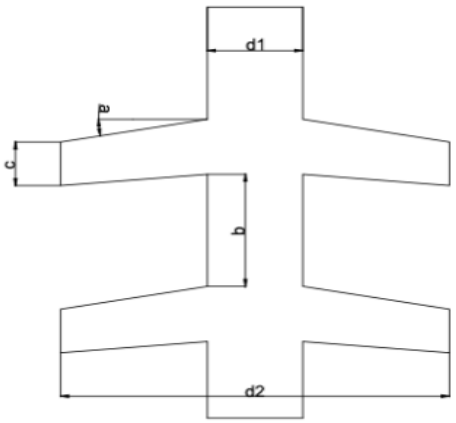

Fig. 5. Rod insulator model.

According to formula (13) and Figure 5, the leakage current limit is determined by the diameter of the insulator body d1, since this is the diameter at which the arc can develop at the lowest current. For the arc to extend at the edge of the rib (d = d2), a much higher current is required. After flashovering, the ribs of the insulator along the arc reference bar slide freely along the surface of the adjacent ribs up to their edges, as this movement leads to a decrease in the resistance of the circuit and, accordingly, to an increase in the current and a further decrease in the resistance of the arc (while its length remains unchanged) [42]. Therefore, the wet discharge voltage for a ribbed insulator is equal to

$$U_{MD} = I_{ls}R_s = (\alpha\pi\gamma_s d_1)^{1/(1+n)} \cdot$$
$$\cdot\left(\frac{bm}{\alpha\pi\gamma_s d_1} + \frac{cm}{\alpha\pi\gamma_s d_2} + \frac{m}{\alpha\pi\gamma_s \cos\alpha}\ln\frac{d_2}{d_1}\right) =$$
$$= \frac{a^{1/(1+n)}mb}{(\pi\gamma_s d_1)^{n/(1+n)}}\left(1 + \frac{c}{b}\cdot\frac{d_1}{d_2} + \frac{d_1}{b\cos\alpha}\ln\frac{d_2}{d_1}\right),$$

where m – is the number of ribs of the insulator.

MOISTURE DISCHARGE VOLTAGE CALCULATION TOOL

With approximate results from method one and formulas from an alternative method using commonly known data for calculation, it is possible to create an automatic wet discharge voltage and insulator voltage calculation tool. In accordance with the formulas from the alternative method, a wet discharge voltage calculation table has been developed (Table 1).

Tab. 1. Calculation results in moisture discharge calculator

Characteristics		Calculated values	
d1, mm	25	Umd, kV	549,08
d2, mm	65	Emd, kV/cm	2,10
b, mm	20		
c, mm	3		
Alfa	12		
L, mm	2610		
H, mm	1055		
γs, mkS	10		
m, st.	29		
type	Ribbed		

Where d1 – is the diameter of the insulator bar, d2 – is the diameter of the insulator cap, b – is the height of the gap between the insulator caps, c – is the height of the cap, alfa – is the angle of inclination of the insulator cap, L – is the length of the insulator leakage current, H – is the height of the insulator, γп – is the conductivity of the pollution layer, m – the number of caps along the length of the insulator rod, type – depending on the diameter of the caps, it can be ribbed (with the same diameter of caps along the entire length of the insulator) or complex (with caps of different diameters). The basis for the calculations and initial data is the insulator database, which is a table of insulator characteristics (Table 2). By introducing new insulators into this database, it is possible to obtain moisture discharge characteristics. The technical characteristics are given in the technical documentation of the respective insulator. A separate calculation sheet is used for the calculation. It contains calculations for the complex and simple shapes of insulators according to the formulae given above. A number of auxiliary functions have also been implemented, such as the calculation of the limiting leakage current, the calculation of the wet discharge voltage and others. According to the results of the calculations, it was found that with a conductivity of the contamination layer of 10 μS for the polymer insulator LK 70-110, the wet discharge voltage was 549 kV, which corresponds to a wet discharge voltage of 2.1 kV/cm of the leakage current path length.

EXPERIMENT TO VERIFY THE CALCULATION RESULTS

To verify the above-described means of calculating the moisture discharge voltage, it was decided to conduct a series of experiments in a large high-voltage hall of NTU 'KHPI'.

Since the available laboratory equipment did not allow us to technically realize the testing of polymer insulators of interest with nominal voltage of 110 kV, it was decided to proceed from the results obtained in the first method. According to it, the average moisture discharge voltage for a 50 Hz network will be from 2.1 to 2.4 kV/cm.

Before conducting the experiment, the test transformer was pre-calibrated.

The voltage on the high side of the transformer was measured using a 6.25 cm diameter ball measuring arrester connected through a protective water resistance (380 Mohm), according to GOST 17512-82.

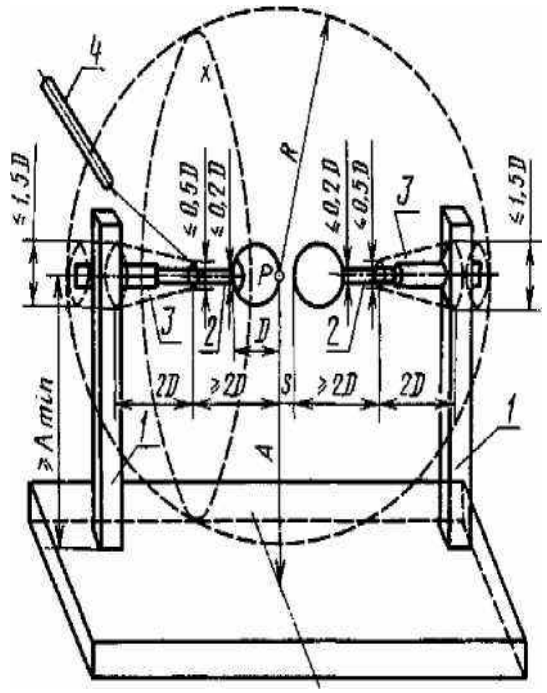

Fig. 6. Sketch of the measuring device.

Measurements of high voltage were carried out at distances between balls 2,8 cm ;4 cm ;5 cm. That corresponds according to GOST 17512-82 76 kV; 95 kV; 107 kV. The obtained results are approximated by a linear function.

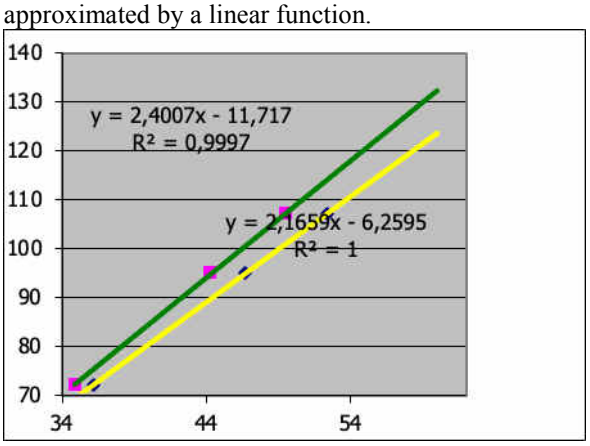

Fig. 7. Measurement results.

The polymer support insulator IOSK 20-20-280-2 with a leakage path length of 620 mm was selected for testing.

Since there was no technical possibility to determine the conductivity of the contamination layer in the laboratory, it was decided to create an artificial contamination, however close to real conditions and corresponding to the maximum.

To create a uniform layer of dust on the surface of the new insulator, it was left in the outdoor storage rooms of the university for some time.

The insulator was then sprayed liberally with a spray gun to simulate precipitation.

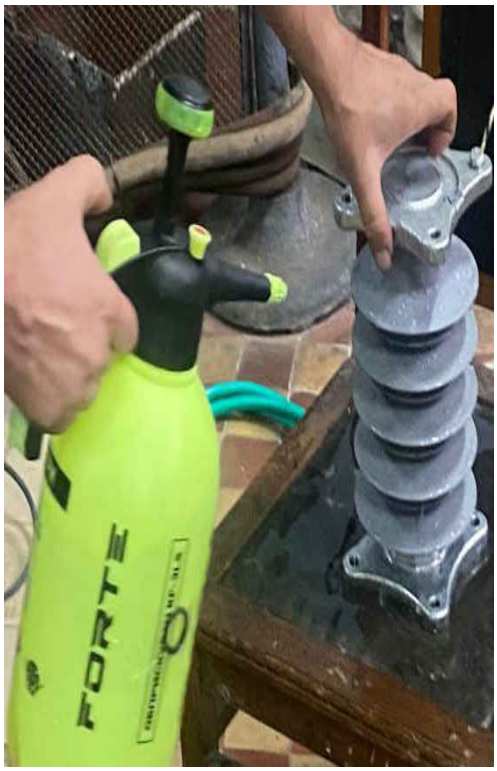

Fig. 8. Preparing the sample for the experiment.

After preparation, voltage was gradually applied to the insulator body. The experiment was accompanied by video recording and the measuring instruments had a maximum value recording function, which allowed the data to be saved after the automatic shutdown of the equipment.

Fig. 9. Overlapping of the moistened insulator.

During the experiment, it was found that the moisture discharge voltage for this insulator ranged from 142 kV to 146 kV, which is 2.29 and 2.35 kV/cm for the above-mentioned leakage path length.

A similar experiment was also carried out for porcelain insulator C4-80-II-M UHL 1. The results of the experiment are shown in Figure 10.

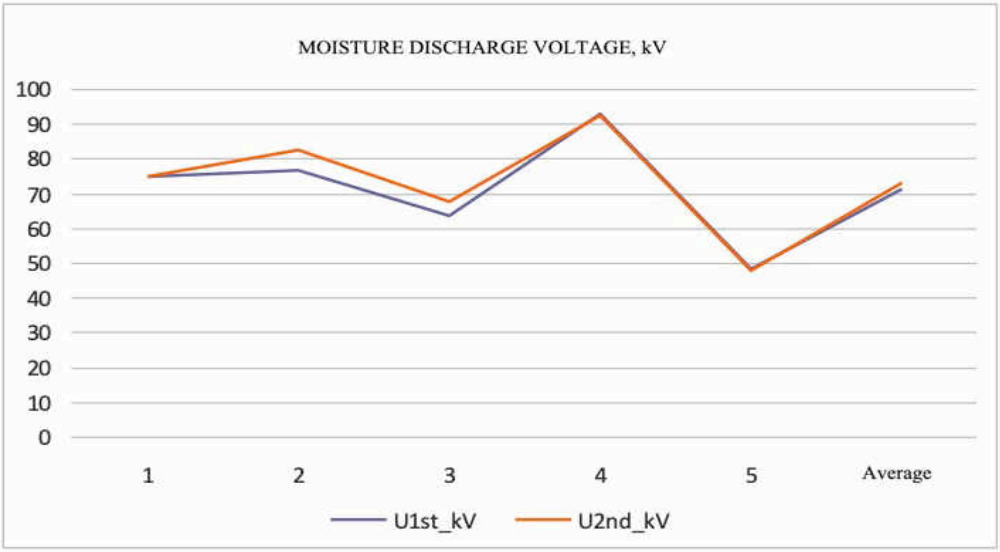

Fig. 10. Experimental results for insulator C4-80-II-M.

For this insulator, the average value of the moisture discharge voltage was 71 kV/cm, which, with a leakage path length of 300 mm, gives a moisture discharge voltage of 2.37 kV/cm. These data are also in agreement with those obtained in the calculation.

CONCLUSION

The results of the calculation fully agree with the results of the determined mean value of the wet discharge voltage, with a value of 2.1 to 2.5 kV/cm, which confirms that the alternative method gives valid values in the calculation. Therefore, it can be concluded that this tool is well suited for the calculation of moisture discharge characteristics and its results can be used for comparison with experimental values. It should be noted that this technique was primarily developed to determine the moisture discharge characteristics of insulators with an external location, but this does not make it unsuitable for use in the calculation of insulators in the conditions of an underground substation. The main difference will be the relative constancy of the humidity of the contamination on the insulators and the nature of the contamination, which will not have a chaotic growth as with the external location of the equipment, but rather a linear one. These issues require a detailed study, which will be the subject of our next work.

To confirm the accuracy of the chosen calculation methodology, a number of experiments were carried out. The obtained data with a high degree of accuracy correspond to the specified data in the first methodology and largely coincide with the results of the calculation carried out according to the second methodology.

Литература (References)

[1] Cao W., Zhang M., Liu Q., et al., “The effect of moisture at the composite interface of cable joint on its flashover characteristics,” High Voltage Technol. 44(11), 3699–3706 (2018).

[2] ASTM D2144-07. (2013). Standard Practices for Examination of Electrical Insulating Oils by Infrared Absorption. ASTM International, West Conshohocken, PA.

[3] Chen H., Zhao H. Investigating the impact of water uptake and sheath moisture on electric field distribution in internal air gaps of high voltage composite insulators. In Journal of Physics: Conference Series, 2025, Vol. 2936, No. 1, p. 012034.

[4] Forrest, J. S. The characteristics and performance in service of highvoltage porcelain insulators. Journal of the Institution of Electrical Engineers-Part II: Power Engineering, 1942, 89.7: 60-80.

[5] IEEE Std 1125-1993: IEEE Guide for Moisture Measurement and Control in SF6 Gas-Insulated Equipment (1993). Place of publication not identified: IEEE. Available at: https://doi.org/10.1109/IEEESTD.1993.8684475.

[6] Konig D., "Problem der Isoliergasfeuchte in metalgekapselten Hochspannungs-Schaltanlagen", ETZA, Bd. 94, H. 7, S. 384-390, 1973.

[7] Kirichenko M.V., Zaitsev R.V., Dobrozhan A.I., et. al., “Adopting of DC magnetron sputtering method for preparing semiconductor films”, 2017 IEEE International Young Scientists Forum on Applied Physics and Engineering, Lviv, Ukraine, 2017. DOI: 10.1109/YSF.2017.8126600

[8] Cheng T., Ji L., Su P., Li Y., Li G., Jiang X., Wang L. Experimental Research on the Impact of Water Vapor and Solid Particles on the Air Gap DC Discharge Characteristics. In Frontier Academic Forum of Electrical Engineering, Springer, Singapore, 2025, pp. 213-221.

[9] Nitta T., Shibuya Y., Fujiwara Y., Arahata Y., Takahashi H., Kuwahara H. "Factors Controlling Surface Flashover in SF6 Gas Insulated Systems," Power Apparatus and Systems, IEEE Transactions on, vol. PAS97, no.3, pp.959 - 968, May 1978.

[10] Nguyen T. P., Cho M. Y. A cloud-based leakage current classified system for high voltage insulators with improved particle swarm optimization and hybrid deep learning technique. Engineering Applications of Artificial Intelligence, 2025, 143, 109987.

[11] Jingyan L. I., et al. Use of leakage currents of insulators to determine the stage characteristics of the flashover process and contamination level prediction. IEEE Transactions on Dielectrics and Electrical Insulation, 2010, 17.2: 490-501.

[12] Kreuger F. H., “Industrial High Voltage”. ISBN 978-90- 6275-561-5, Delft University Press 1991.

[13] CIGRÉ working group A2.30, Technical Brochure 349, “Moisture Equilibrium and Moisture Migration within Insulation Systems”, 2008.

[14] Borzenkov I. I., et al. Investigation of the leakage current of the suspend dish insulator of type PSD-70E in various conditions. In: 2020 IEEE 4th International Conference on Intelligent Energy and Power Systems (IEPS). IEEE, 2020. p. 98-101.

[15] Zhang Z., Yang F., Zhang H., Zhou C., Li Y., Liu H. A probabilistic neural network assessment method for insulator pollution level based on discharge noise. Measurement, 2025, 242, 115869.

[16] Gençoğlu M. T., Cebeci M. The pollution flashover on high voltage insulators. Electric

Power Systems Research, 2008, 78.11: 1914-1921.
[17] Schneider H. M., Turner F. J. Switching surge flashover characteristics of long sphere-plane gaps of UHV station design. PAS-94, 1972, No 2, p. 551--559.
[18] Youping T. U., et al. Effect of moisture on temperature rise of composite insulators operating in power system. IEEE Transactions on Dielectrics and Electrical Insulation, 2015, 22.4: 2207-2213.
[19] Gielniak J., Graczkowski A., Moranda H., Przybylek P., Walczak K., Nadolny Z., Moscicka-Grzesiak H., Feser K., Gubanski S. M. "Moisture in cellulose insulation of power transformers-statistics", IEEE TDEI, Vol. 20, No. 3, pp. 982- 987, 2013.
[20] Zhijin Z., et al. Study on the wetting process and its influencing factors of pollution deposited on different insulators based on leakage current. IEEE Transactions on Power Delivery, 2013, 28.2: 678-685
[21] Sun F., Jing F., Wang J., Li X., Zhai Z., Liu X., Chu J. Breakdown Characteristics and Decomposition Mechanisms of Air-Insulation Mediums in High-Altitude Conditions. In Frontier Academic Forum of Electrical Engineering, Springer, Singapore, 2025, pp. 163-173.
[22] Sangkasaad S. Research and experience with new insulator technologies in Thailand // Proceeding of 2001 World insulator congress: applying new technologies for better reliability and lower costs. – Shanghai, 2001. – pp. 154-167.
[23] Dai Z., Wang D., P. Jarman P. "Creepage Discharge on Insulation Barriers in Aged Power Transformers", IEEE TDEI, Vol. 17, No. 4, pp. 1327- 1335, 2010.
[24] Haibo L., Yuming Z., Guowei L., Shiyong J., Zhengjia Z. Energy efficiency comparison of AC and DC distribution systems in commercial buildings based on time series simulation. J. Electrotech. 2020, 35, 4194–4206.
[25] Zeng S., Zhao X., Li W., Peng Y., Liu Y., Yan X., Zhang G. Performance comparison and lifespan assessment of naturally and artificially chalked silicone rubber for composite insulators. Polymer Degradation and Stability, 2025, 232, 111139.
[26] Fahmi D., Asfani D. A., Hernanda I. G. N. S., Septianto B., Negara I. M. Y., Illias H. A. Partial discharge characteristics from polymer insulator under various contaminant. Electric Power Systems Research, 2024, 236, 110978.
[27] Liao J., Zhou N., Wang Q., Li C., Yang J. Definition and correlation analysis of power quality indicators of DC distribution network. Chin. J. Electr. Eng. 2018, 38, 6847–6860+7119
[28] Jung J. H., Kim H. S., Ryu M. H., Baek J. W. Design methodology of bidirectional CLLC resonant converter for high-frequency isolation of DC distribution systems. IEEE Trans. Power Electron. 2013, 28, 1741–1755.
[29] Gollee R., Gerlach D. An FEM-Based Method for Analysis of the Dynamic Behavior of AC Contactors. IEEE Trans. Magn. 2000, 36, 1337–1340.
[30] Tarra J. R., Guntreddi V. R., Suneeta K., Suman J. V., Gorripotu T. S., Kanthi A. Qualitative Analysis on Impact of Aging on the Electrical Properties of Polymeric Insulators. In 2024 International Conference on Advances in Modern Age Technologies for Health and Engineering Science (AMATHE), 2024, pp. 1-6.
[31] Minfu L., Jinqiang H., Guowei G., Shanjun W., Xiongying D. Development and research status of hybrid circuit breaker at home and abroad. High Volt. Eng. 2016, 42, 1688–1694
[32] Shimin X., Chaochao C., Yi J., Jian S., Tao W., Jiali H., Ying W. A Summary of Research on DC Distribution System Protection Technology. Proc. Chin. Soc. Electr. Eng. 2017, 37, 966–978
[33] Koch M., Tenbohlen S., Stirl T., "Diagnostic Application of Moisture Equilibrium for Power Transformers", IEEE Trans. Power Delivery Vol. 25, No. 4, pp. 2574- 2581, 2010
[34] Luhui L., Zhihao Y., Lijun F., Youxing X., Nan W. Research & Development Status and Prospects of Fast DC Circuit Breakers. Proc. Chin. Soc. Electr. Eng. 2017, 37, 966–978.
[35] Barbosa V. R., Lira G. R., Costa E. G., Galdino G. M., Oliveira A. H., Júnior A. C. S. Estimation of the Pollution Critical Level on the Surface of Glass Insulators Based on Leakage Current. IEEE Transactions on Power Delivery, 2024.
[36] Junjia H., Zhao Y., Wenting Z., Shai F., Xinlin Y., Huan P. Summary of technology development of DC Breaker Technology. South Power Syst. Technol. 2015, 9, 9–15
[37] Xiaoguang W., Bingjian Y., Guangfu T. Technology Development and Engineering Practice of High Pressure DC Breaker Technology. Power Syst. Technol. 2017, 41, 1319–1323
[38] Leibfried T., Thieb U., Hohlein I., Breitenbauch B., Lainck T., Leibner J., Truant S. "Profile of Water Content and Degree of Polymerisation in the Solid Insulation of Power Transformers", IEEE Intern. Sympos. Electr. Insul. (ISEI), Indianapolis, USA, pp.109- 112, 2004.
[39] Shede P., Mane S. Leakage current sensing techniques. In Proceedings of the 2017 Third International Conference on Sensing, Signal Processing and Security (ICSSS), Chennai, India, 4–5 May 2017; pp. 181–185.
[40] Kudo T., Kuribara S., Takahashi Y. Wide-range AC/DC earth leakage current sensor using fluxgate with self-excitation system. In

Proceedings of the SENSORS, 2011 IEEE, Limerick, Ireland, 28–31 October 2011; pp. 512–515.

[41] Xiao J., Wang P., Setyawan L. Hierarchical Control of Hybrid Energy Storage System in DC Microgrids. IEEE Trans. Ind. Electron. 2015, 62, 4915–4924.

[42] Palangar M. F., Mirzai M., Mahmoudi A. Improved flashover mathematical model of polluted insulators: A dynamic analysis of the electric arc parameters. Electric Power Systems Research, 2020, 179: 106083.

Сведения об авторах.

Prof. **Serhii Yuriyovych Shevchenko**
Doctor of Technical Science
Department of electric power transmission
Research interests: Electricity transmission, protection of electric power facilities.
E-mail: sergii.shevchenko@khpi.edu.ua

Dr. Dmytro Oleksiyovych Danylchenko
Ph. D. of Technical Science
Department of electric power transmission
Research interests: Electricity transmission, protection of electric power facilities,
E-mail: dmytro.danylchenko@khpi.edu.ua

Roman Oleksiyovych Hanus,
Department of electric power transmission
Research interests: Electricity transmission, protection of electric power facilities, underground power grids.
E-mail: roman.hanus@ieee.khpi.edu.ua

Dr. **Serhii Anatoliyovych Radohuz**
Research interests encompass a broad spectrum of fields, reflecting a dedication to both contemporary and historical perspectives. Renewable energy sources are another critical domain of interest.
E-mail: serhii.radohuz@khpi.edu.ua

Prof. Roman Serhiyovych Tomashevskiy,
Doctor of Technical Science
Research interests: Distributed generation, renewable sources, AI in object and process control
E-mail: roman.tomashevskyi@khpi.edu.ua

Dr. Mykola Vitaliyovych Makhonin
Ph. D. of Technical Science
Research interests: Electricity transmission, protection of electric power facilities, renewable sources, AI in object and process control
E-mail: mykola.makhonin@khpi.edu.ua

Andrii Eduardovych Potryvai
Department of electric power transmission
Research interests: Electricity transmission, distributed generation, renewable sources,
E-mail: andrii.potryvai@ieee.khpi.edu.ua